2016

R134a Flow Boiling inside a 4.3 mm ID Microfin Tube

Simone Mancin
Dept. of Management and Engineering, University of Padova, Italy, simone.mancin@unipd.it

Claudio Zilio
Dept. of Management and Engineering, University of Padova, Italy, claudio.zilio@unipd.it

Giulia Righetti
Dept. of Management and Engineering, University of Padova, Italy, righetti@gest.unipd.it

Luca Doretti
Dept. of Civil, Architectural and Environmental Engineering, University of Padova, Italy, luca.doretti@unipd.it

Giovanni A. Longo
Dept. of Management and Engineering, University of Padova, Italy, tony@gest.unipd.it

R134a Flow Boiling inside a 4.3 mm ID Microfin Tube

Simone MANCIN[1*], Claudio ZILIO[1], Giulia RIGHETTI[1], Luca DORETTI[2], Giovanni A. LONGO[1]

[1] Dept. of Management and Engineering,
University of Padova, Str.lla S. Nicola, 3, VICENZA, 36100-Italy
simone.mancin@unipd.it, claudio.zilio@unipd.it, righetti@gest.unipd.it, tony@gest.unipd.it

[2] Dept. of Civil, Architectural and Environmental Engineering,
University of Padova, Via Venezia, 1 PADOVA – 35131, Italy
luca.doretti@unipd.it
* Corresponding Author

ABSTRACT

The minimization of the refrigerant charge in refrigerating and air conditioning equipment is an important issue due to the new environmental challenges. Recently, relatively small smooth copper tubes with outer diameter around 5 mm have been implemented in many air conditioning and refrigeration equipment. Since their introduction in late 1970s, microfin tubes have also been largely used to enhance both single and two-phase heat transfer. This paper presents R134a flow boiling heat transfer and pressure drop measurements inside a mini microfin tube with internal diameter of 4.3 mm. The microfin tube was brazed inside a copper plate and electrically heated from the bottom by means of a wire resistance. Several T-type thermocouples were inserted in the wall to measure the temperature distribution during the phase-change process. In particular, the experimental measurements were carried out at constant inlet saturation temperature of 30 °C, by varying the refrigerant mass velocity between 100 kg m^{-2} s^{-1} and 800 kg m^{-2} s^{-1}, and the vapor quality from 0.1 to 0.95 at four different heat fluxes: 15, 30, 60 and 90 kW m^{-2}. The experimental results are presented in terms of two-phase heat transfer coefficient, vapor quality at the onset of dryout, and frictional pressure drop.

1. INTRODUCTION

Since the invention of Fujie *et al.* (1977), microfin tubes have received a lot of attention because they can assure higher heat transfer coefficients compared to smooth tubes, with a relatively small increase of pressure drop. In addition, by means of the fins along the circumference of the tube, microfin tubes facilitate the transition to annular regime, with consequent higher heat transfer coefficient than those during stratified regimes. Furthermore, the vapor quality at the onset of the dryout phenomenon is delayed.

Over the last decades, traditional microfin tubes were largely studied, during both flow boiling and condensation. Experimental results regarding heat transfer coefficient, pressure drop, and vapor quality at the onset of the dryout are now available, as well as flow pattern maps and empirical equations for the estimation of those parameters, which can be used to design evaporators and condensers commonly used in traditional air conditioning and refrigeration systems. More recently, microfin tubes with internal diameter smaller than 5 mm are becoming more and more popular because they can be used in the next generation of air conditioning and refrigeration systems, leading to more compact and more efficient heat exchangers. Furthermore, the use of these mini microfin tubes may imply a large reduction of the refrigerant charge of the system, thus facing with the new stricter environmental regulations. For these reasons, large manufacturers are exploring the possible use of mini microfin tubes and there is a strong interest in understanding the heat transfer and pressure drop behaviors of these enhanced tubes.

The literature about small diameter microfin tubes (i.e. inner diameter lower than 6 mm or so) is poor if compared with larger tubes. Among the most recent works, Kondou *et al.* (2013) investigated R32, R1234ze(E), and two R32/R1234ze(E) mixtures (20:80 and 50:50 by wt%) flow boiling inside a water heated microfin tube (inner diameter at the fin tip of 4.94 mm) at a saturation temperature of 10 °C, heat fluxes of 10 and 15 kW m^{-2}, and mass velocities from 150 to 400 kg m^{-2} s^{-1}.

Kondou *et al.* (2014a) also investigated R1234ze(Z) during flow boiling inside the same microfin tube at different saturation temperatures from 0 to 30 °C and at a fixed heat flux equal to 10 kW m^{-2}. The Authors reported the experimental results relative to three different refrigerant mass velocities, 150, 200, and 300 kg m^{-2} s^{-1}; the results showed that the heat transfer coefficients of R1234ze(Z) were slightly higher than those of R1234ze(E) and R134a at vapor quality values from 0.4 to the thermal crisis while they were slightly lower for vapor qualities lower than 0.4.
Furthermore, Kondou *et al.* (2014b) investigated the boiling performance of high temperature glide refrigerant mixtures containing R1234ze(E) in blend with R744 and R32 (R744/R32/R1234ze(E), 4:43:53 and 9:29:62 by wt%) inside the same water heated microfin tube, at 10 °C of saturation temperature, 10 kW m^{-2} of heat flux and mass velocity ranging from 150 to 600 kg m^{-2} s^{-1}. The Authors compared the boiling results obtained for the ternary mixture with those of the pure fluids and with those obtained for other two binary mixtures of R32/R1234ze(E) (30:70 and 40:60 by wt%). The heat transfer coefficients of the binary and ternary blends were drastically lower than those measured for the pure refrigerants because of the large mass transfer resistance, which seemed to suppress both the nucleate and forced convective contributions.
Diani *et al.* (2014) compared R1234ze(E) against R134a in a 3.4 mm ID at the fin tip electrically heated microfin tube at 30 °C of saturation temperature by varying the mass velocity from 190 to 940 kg m^{-2} s^{-1} and the heat flux from 10 to 50 kW m^{-2}. The results showed that the flow boiling heat transfer coefficients measured for R1234ze(E) were lower, at least similar, to those for R134a, while the two refrigerants showed similar critical values of vapor quality and heat flux. The same Authors (Diani *et al.*, 2015a) measured the flow boiling performance of R1234yf inside the same mini microfin tube at 30 °C of saturation temperature. The Authors investigated the effects of the mass velocity, vapor quality, and heat flux and then compared the experimental data with that measured for R134a (Mancin *et al.*, 2015).
Diani *et al.* (2015b) and Diani and Rossetto (2015) studied R1234ze(E) and R1234yf and R134a, respectively, flow boiling inside a 2.4 mm microfin tube at 30 °C of saturation temperature, mass velocity from 375 to 940 kg m^{-2} s^{-1}, and heat flux from 10 to 50 kW m^{-2}. For the R1234ze(E), the Authors found that at low heat flux, the heat transfer coefficient was highly affected by vapor quality, meaning that two phase forced convection was the mechanism which mainly controls the flow boiling phenomenon. A different situation was found at high heat fluxes, where the heat transfer coefficient was not affected by mass velocity and weakly affected by vapor quality, meaning that the flow boiling process was mainly controlled by nucleate boiling
Despite the recent work dealing mainly with HFOs listed above, the database for boiling of refrigerants inside relatively small diameter microfin tubes is still limited and new data is surely useful for the proper assessment of this type of tubes.
This paper presents an experimental work about flow boiling of one of the still most widely used refrigerant, R134a inside mini microfin tube having a fin tip diameter of 4.3 mm. The measurements were carried out by varying mass velocity from 100 to 800 kg m^{-2} s^{-1}, heat flux from 15 to 90 kW m^{-2}, at a constant inlet saturation temperature of 30 °C. The results permit to highlight the effects of the operative working conditions such as vapor quality, heat flux, and mass velocity, on the thermal and hydraulic behavior of the mini microfin tube under investigation.

2. EXPERIMENTAL SETUP AND TEST SECTION

The experimental setup is located at the Nano Heat Transfer Lab (NHT-Lab) at the Department of Management and Engineering of the University of Padova. As shown in Figure 1, the experimental facility consists of three loops: refrigerant, cooling water, and hot water loops. The rig was designed for heat transfer and pressure drop measurements and flow visualization during either vaporization or condensation of pure refrigerants and refrigerants mixtures inside structured micro- and nano-geometries.
The refrigerant is pumped through the circuit by means of a magnetically coupled gear pump, then it is vaporized in a Brazed Plate Heat Exchanger (BPHE) fed with hot water to achieve the desired value of vapor quality. The hot water is supplied by a thermostatic bath; both water flow rate and water temperature can be independently set. The heat flow rate exchanged at the BPHE evaporator is accurately measured by means of a magnetic flow meter and a calibrated T-type thermopile; furthermore, preliminary tests were run to verify the heat balance between refrigerant and water sides, the results showed a misbalance always less than 2%. The refrigerant enters the microfin test tube at a known mass velocity and vapor quality and then it is vaporized by means of a calibrated Ni-Cr wire resistance. The electrical power supplied to the sample is indirectly measured by means of a calibrated reference resistance (shunt) and by the measurement of the effective electrical difference potential of the resistance wire inserted in the copper heater. The current can be calculated from the Ohm's law. The fluid leaves the test section and enters in a post-condenser, a brazed plate heat exchanger fed with tap water, where it is fully condensed and subcooled. A damper connected to the compressed air line operates as pressure regulator to control the saturation conditions in the refrigerant loop.

Table 1: Instruments uncertainty.

Transducer	Uncertainty (k=2)
T-type thermocouples	± 0.1 K
T-type thermopiles	± 0.05 K
Electric power	± 0.26% of the reading
Coriolis mass flowmeter (refrigerant loop)	± 0.10% of the reading
Magnetic volumetric flowmeter (hot water loop)	± 0.2% of FS= 0.33 10^{-3} m^3 s^{-1}
Differential pressure transducer (test section)	± 0.075% of 0.3 MPa
Absolute pressure transducers	± 0.065% of FS= 4 MPa

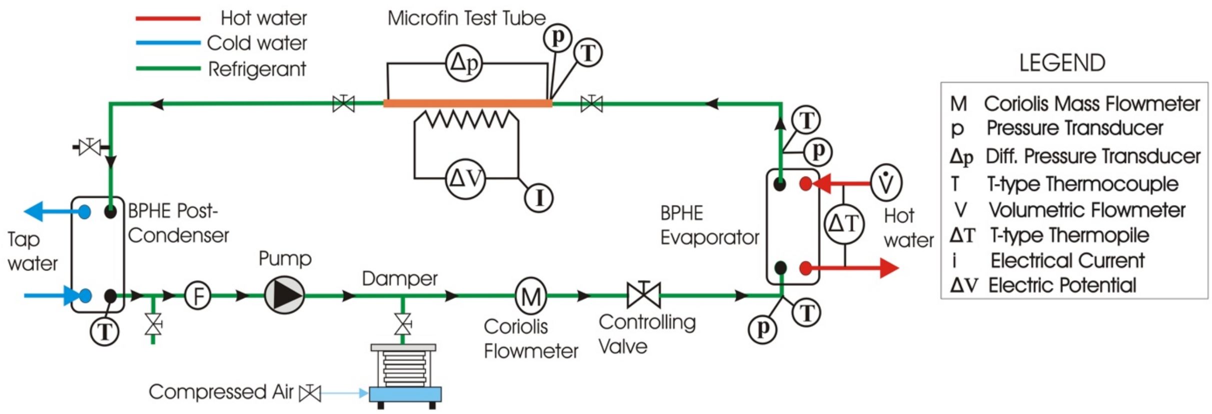

Figure 1: Schematic of the experimental setup.

As shown in Figure 1, the refrigerant pressure and temperature are measured at several locations throughout the circuit to know the refrigerant properties at the inlet and outlet of each heat exchanger. The refrigerant mass flow rate can be independently controlled by the gear pump and it is measured by means of a Coriolis effect flowmeter. No oil circulates in the refrigerant loop. Table 1 lists the values of uncertainty (k=2) of the instruments used in the experimental facility. The mini microfin tube was brazed inside a guide milled on the top surface of a copper plate, which is 200 mm long, 10 mm wide, and 20 mm high. 16 holes were drilled just 1 mm below the microfin tube, in order to locate as many T-type thermocouples to monitor the wall temperature distribution. Another guide was milled on the bottom side of the copper plate, to host a Nickel-Chrome wire resistance connected to a DC current generator, which supplies the heat flow rate needed to vaporize the refrigerant flowing inside the tube. In order to avoid the abrupt pressure drops due to flow contraction and expansion, a suitable smooth connection to the refrigerant circuit having the same fin tip diameter (D=4.3 mm) was designed and realized to join the test tube with inlet and outlet pipes. Pressure ports are located about 25 mm downstream and upstream of the copper plate, thus the length for pressure drop measurements is 250 mm.

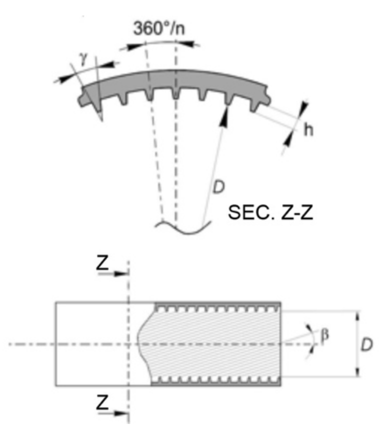

Figure 2: Schematic of a microfin tube.

Table 2: Microfin tube geometry.

Characteristic	Value
Outer diameter, OD	5.0 mm
Fin tip diameter, D	4.3 mm
Apex angle, γ	11°
Helix angle, β	27°
Number of fin, n	54
Fin height, h	0.12 mm
Tube thickness, t	0.23 mm

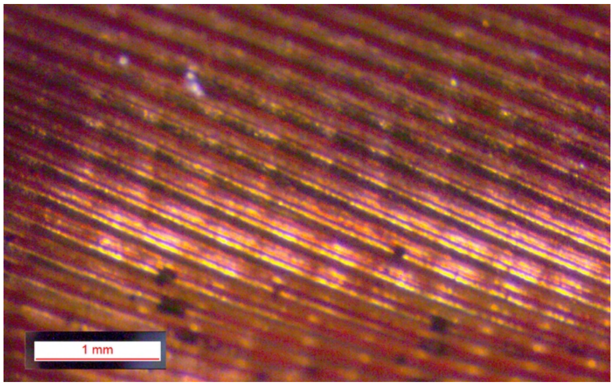

(a)

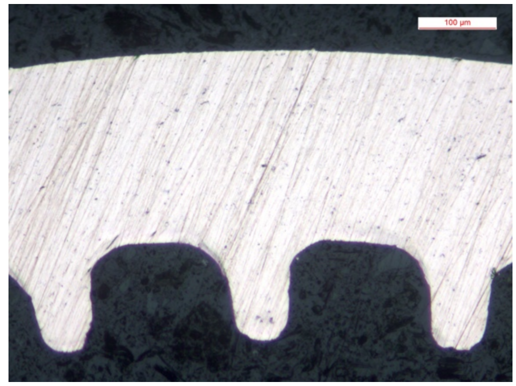

(b)

Figure 3: Photos of longitudinal view (a) and of a cross section (b) of the tested microfin tube.

The test section is located inside an aluminum housing filled with 15 mm thick ceramic fiber blanket, to limit as much as possible the heat losses due to conduction to the ambient. Figure 2 and Table 2 summarize the main geometrical characteristics of the tested tube. Given the reported dimensions, the area enhancement with reference to the smooth tube having the same fin tip diameter is equal to 1.87. Figure 3 reports two photos of the tested microfin tube where one can clearly observe the helical fins (a) and their cross section (b).

3. DATA REDUCTION

As described in the previous section, the subcooled liquid pumped by the magnetically coupled gear pump is vaporized into a BPHE fed with hot water. Thus, the vapor quality at the inlet of the test section can be calculated from a thermal balance at the evaporator, as:

$$q_{evap} = \dot{m}_w \cdot c_{p,w} \cdot \left(t_{w,in} - t_{w,out}\right) = \dot{m}_r \cdot \left(J_{in,TS} - J_{L,sub}\right) \tag{1}$$

where $\dot{m}_w$ is the water mass flow rate, $c_{p,w}$ is the specific heat capacity of the water, $t_{w,in}$ and $t_{w,out}$ are the inlet and outlet water temperatures. The right-hand side term of eq. (1) reports the refrigerant side heat flow rate where $\dot{m}_r$ is the refrigerant mass flow rate while $J_{in,TS}$ and $J_{L,sub}$ are the unknown specific enthalpy at the inlet of the test section and the specific enthalpy of the subcooled liquid entering the BPHE, respectively. Once calculated $J_{in,TS}$, the vapor quality at the inlet of the test section can be estimated by:

$$x_{in,TS} = \frac{J_{in,TS} - J_L}{J_V - J_L} \tag{2}$$

where J_L and J_V are the specific enthalpies of the saturated liquid and vapor, respectively, evaluated at the saturation pressure of the refrigerant measured at the inlet of the test section. As already described, the electrical power supplied to the sample is indirectly measured by means of a calibrated reference resistance (shunt) and by the measurement of the effective electrical difference potential of the resistance wire inserted in the copper heater.

Preliminary heat transfer measurements permitted to estimate the heat loss (q_{loss}) due to conduction through the test section as a function of the mean wall temperature. The tests were run under vacuum conditions on the refrigerant channel by supplying the power needed to maintain the mean wall temperature at a set value. The measurements were carried out by varying the mean wall temperature from 28 °C to 63 °C. The results show that the heat loss increases linearly as the mean wall temperature increases (R>0.99). In the tested range of wall temperature, the heat loss by conduction through the test section can be estimated by:

$$|q_{loss}| = 0.2006 \cdot \bar{t}_{wall}\ [°C] - 4.6698 \quad [W] \tag{3}$$

thus, the actual heat flow rate q_{TS} supplied to the sample is given by:

$$q_{TS} = P_{EL} - |q_{loss}| = \Delta V \cdot I - |q_{loss}| \tag{4}$$

It is worth underlying that the q_{loss} varied from 2.5% to 4% of the electrical power supplied. The specific enthalpy at the outlet of the test section can now be calculated from:

$$q_{TS} = \dot{m}_r \cdot \left(J_{out,TS} - J_{in,TS}\right) \tag{5}$$

Hence, the outlet vapor quality is given by:

$$x_{out,TS} = \frac{J_{out,TS} - J_L}{J_V - J_L} \tag{6}$$

where J_L and J_V are the specific enthalpies of the saturated liquid and vapor, respectively, evaluated at the saturation pressure of the refrigerant measured at the outlet of the test section. The mean vapor quality, x_{mean} is the average value between the inlet and outlet ones. The two-phase heat transfer coefficient *HTC*, referred to the nominal area *A*, can be defined as:

$$HTC = \frac{q_{TS}}{A \cdot (\bar{t}_{wall} - \bar{t}_{sat})} = \frac{q_{TS}}{\pi \cdot D \cdot L \cdot (\bar{t}_{wall} - \bar{t}_{sat})} \tag{7}$$

where $\bar{t}_{wall}$ is the average value of the measured wall temperatures $t_{wall,i}$ as:

$$\bar{t}_{wall} = \frac{1}{16} \sum_{i=1}^{16} t_{wall,i} \tag{8}$$

The average value of the saturation temperatures $\bar{t}_{sat}$ is obtained from the measured values of the pressure:

$$\bar{t}_{sat} = \frac{t_{sat,in}(p_{sat,in}) + t_{sat,out}(p_{sat,out})}{2} \tag{9}$$

The hydraulic performance of the microfin tube is given in terms of frictional pressure drop, which was calculated from the measured total pressure drop by subtracting the momentum pressure gradient, as:

$$\Delta p_{\mathrm{f}} = \Delta p_{\mathrm{t}} - \Delta p_{\mathrm{c}} - \Delta p_{\mathrm{a}} \tag{10}$$

The momentum pressure drops are estimated by the homogeneous model for two-phase flow as follows:

$$\Delta p_{\mathrm{a}} = G^2 (v_{\mathrm{V}} - v_{\mathrm{L}})\, |\Delta x| \tag{11}$$

where *G* is the refrigerant mass flux, v_L and v_V are the specific volume of liquid and vapor phase, $|\Delta x|$ is the absolute value of the vapor quality change through the whole test section. The gravitational contribution Δp_{c} was not considered because the microfin tube is horizontally located. Thermodynamic and transport properties are estimated from RefProp v9.1 (Lemmon *et al*., 2013). A detailed error analysis was performed in accordance with Kline and McClintock (1953) using the values of the uncertainty of the instruments listed in Table 1; it was estimated that the uncertainty (k=2) on the two-phase heat transfer coefficient showed a mean value of ±2.1% and a maximum value of ±3.8%, while the uncertainty on the vapor quality was ±0.03. The pressure drops showed a mean uncertainty of around 8%.

3. EXPERIMENTAL RESULTS

This section presents the experimental results collected during vaporization of the R134a inside the mini microfin tube. The saturation temperature at the inlet of the test section was kept constant at 30 °C. This value can be considered suitable for high temperature industrial heat pumps and for electronics cooling applications. The results are given in terms of heat transfer coefficient and frictional pressure gradients, as a function of the operative test conditions, i.e. mean vapor quality, mass velocity, and heat flux.

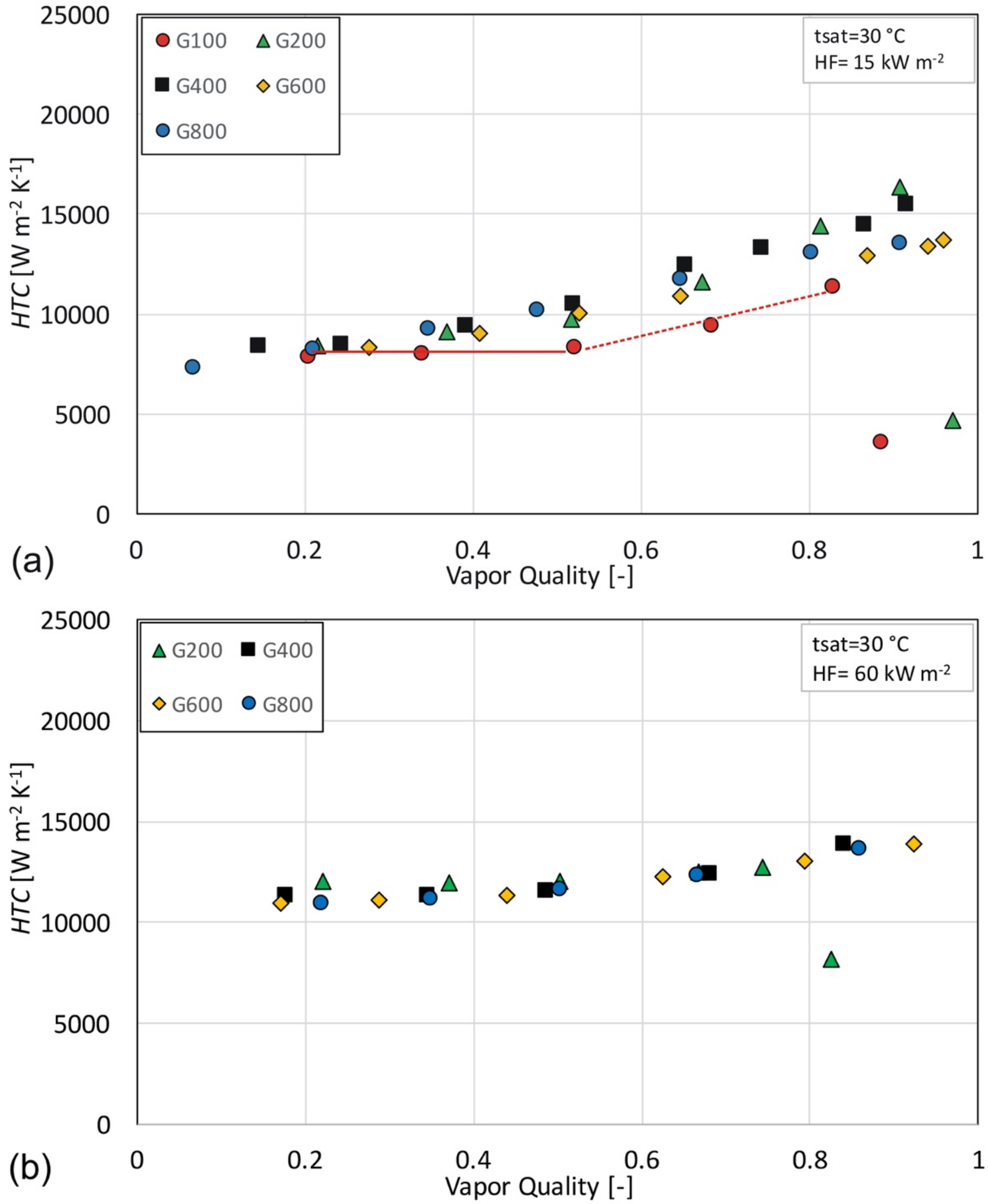

Figure 4: Effect of mass velocity on heat transfer coefficient at two different heat fluxes: HF=15 kW m^{-2} (a) and HF=60 kW m^{-2} (b), G expressed in [kg m^{-2} s^{-1}].

The mass velocity and the heat flux are referred to the cross sectional area and to the heat transfer area, respectively, of an equivalent smooth tube having an internal diameter equal to the diameter at the fin tip of the microfin tube under investigation. The mean vapor quality was varied from 0.1 to 0.95, the mass velocity from 100 to 800 kg m^{-2} s^{-1}, and the heat flux from 15 to 90 kW m^{-2}: in these operating conditions, the vapor quality change through the test section varied from 0.02 to 0.32. The value of Δx=0.32 was considered the maximum acceptable: thus, when increasing the heat flux, one or more refrigerant mass velocities were not collected because they would have presented a higher vapor quality change.

Figure 4 shows the effect of mass velocity on the heat transfer coefficient as a function of the mean vapor quality at two different heat fluxes: HF=15 kW m^{-2} (a) and HF=60 kW m^{-2} (b). In these operating test conditions, the vapor quality changes between inlet and outlet of the test section vary from 0.02 and 0.16 at HF=15 kW m^{-2}, and from 0.08 to 0.32 at HF=60 kW m^{-2}.

The analysis can start at the lowest heat flux (Figure 4a) and from the lowest mass velocity: the heat transfer coefficient remains almost constant at around 8000 W m^{-2} K^{-1} up to a mean vapor quality of 0.5, meaning that the nucleate boiling seems to control the phase change process, whereas at higher vapor qualities it increases, and thus also the two-phase forced convection starts to play a relevant role in the flow boiling phenomenon.

When increasing the mass velocity, the plateau at low vapor quality, where the heat transfer coefficient remains constant, disappears, and the heat transfer coefficient increases almost linearly with the vapor quality, meaning that the two-phase forced convection is mainly affecting in the phase-change process. It is worth pointing out that for x_{mean}<0.3, all the investigated mass velocities show similar values of heat transfer coefficient. Furthermore, at x_{mean} > 0.65, the values of heat transfer coefficient measured at G = 200 kg m^{-2} s^{-1} and G=400 kg m^{-2} s^{-1} are greater than those obtained at higher mass velocities.

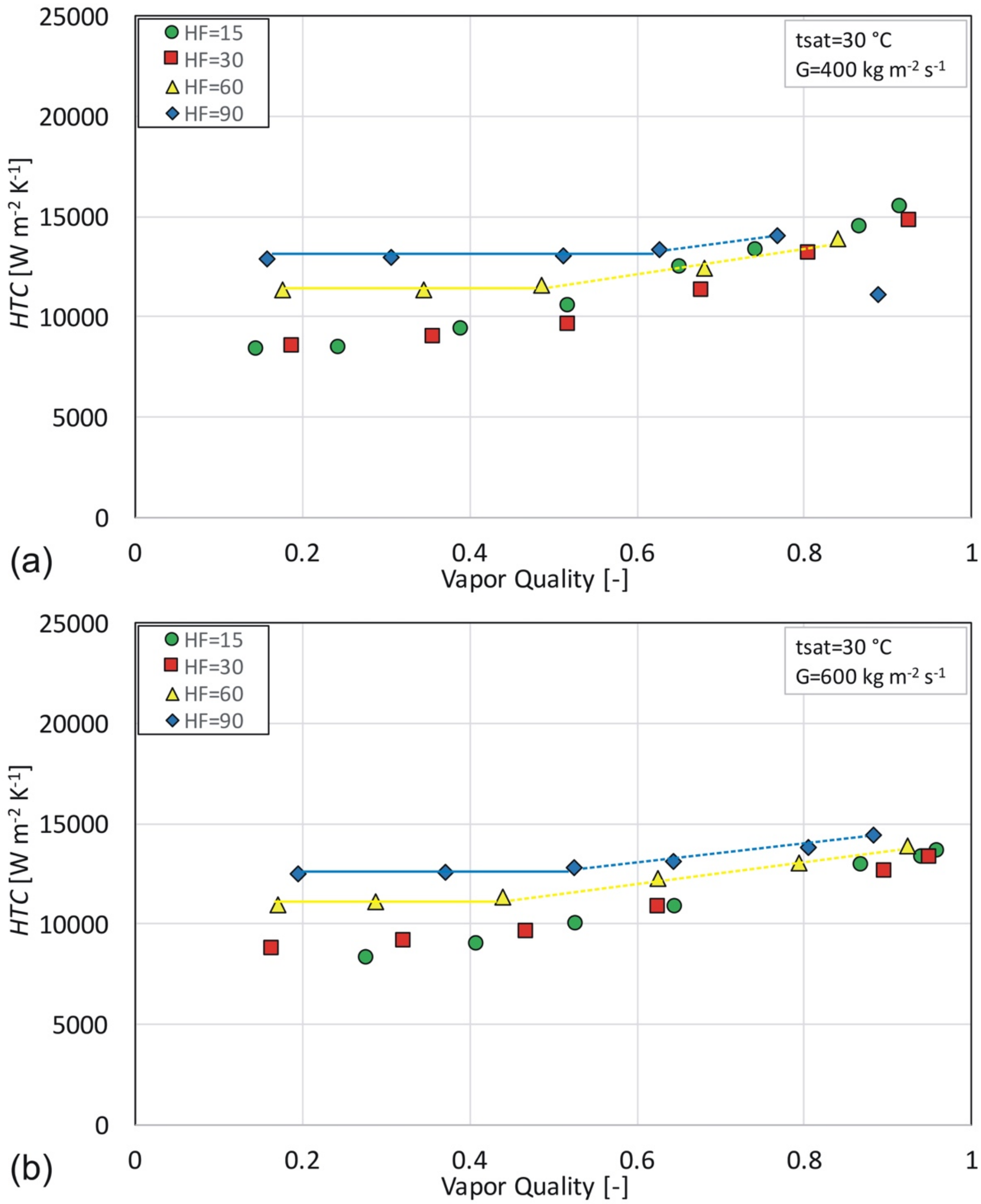

Figure 5: Effect of heat flux on heat transfer coefficient at two different mass velocities: G=400 kg m^{-2} s^{-1} (a) and G=600 kg m^{-2} s^{-1} (b). HF expressed in [kW m^{-2}].

This can be linked to a particular effect induced by the helical microfins that might be emphasized at these operating test conditions. This behavior was also found by Mancin *et al.* (2015) during R134a flow boiling inside a 3.4 mm ID microfin tube. The onset of the dryout was only observed at G=100 kg m^{-2} s^{-1} and G=200 kg m^{-2} s^{-1} and it occurred at around x_{mean}=0.83 and x_{mean}=0.91, respectively.

As reported in Figure 4b, when increasing the heat flux to HF=60 kW m^{-2} slightly different results are found. The two-phase heat transfer coefficients do not show any noticeable effect of the mass velocity: hence, the heat transfer mechanism seems to be controlled by the nucleate boiling. For x_{mean} < 0.5 the heat transfer coefficient, being around 11000 W m^{-2} K^{-1}, is almost constant with the vapor quality at all the investigated mass velocities. As the vapor quality increases, a weak sensitivity on the heat transfer coefficient is shown, which increases as well. The dryout phenomenon was only observed at G=200 kg m^{-2} s^{-1} and the mean vapor quality at the onset of the dryout is around x_{mean}=0.75.

Figure 5 shows the effect of heat flux on heat transfer coefficient at two mass velocities: 400 kg m^{-2} s^{-1} (a) and 600 kg m^{-2} s^{-1} (b). Considering the results depicted in Figure 5a, it can be stated that at heat flux lower than 30 kW m^{-2}, there is not any noticeable effect of this parameter on the boiling heat transfer. In fact, for vapor quality lower than 0.4, the heat transfer coefficients are almost the same; then, for x_{mean}>0.4, the heat transfer coefficient increases and those measured at HF=15 kW m^{-2} become even slightly higher than those collected at HF=30 kW m^{-2}.

This can be explained considering that at these operating conditions, the dominant heat transfer mechanism is the forced convection, which might be also positively influenced by the turbulence induced by the helical microfins, being the helix angle relatively high (β=27°).

It is worth highlighting that when increasing the heat flux, the plateau where the heat transfer coefficient can be considered almost constant, is extended to higher vapor qualities (i.e. to x_{mean}=0.5 and x_{mean}=0.65 for HF=60 kW m^{-2} and HF=90 kW m^{-2}, where the heat transfer coefficients are around 11400 W m^{-2} K^{-1} and 12900 W m^{-2} K^{-1}, respectively). At higher vapor qualities, the heat transfer coefficient slightly increases.

Moreover, at x_{mean}<0.6, for a given vapor quality, the heat transfer coefficient increases as the heat flux increases, especially for HF>30 kW m^{-2}. At these operating conditions, the nucleate boiling can be considered the prevailing phase change mechanism. When the vapor quality becomes higher than 0.65, the heat transfer coefficient profiles converge exhibiting almost the same values. Finally, the dryout was only observed at HF=90 kW m^{-2} confirming the interesting capabilities of the mini microfin tube in delaying the onset of dryout; this characteristic is particularly suitable for electronics cooling application where the dryout event and the consequent sharp surface temperature increase must be avoided.

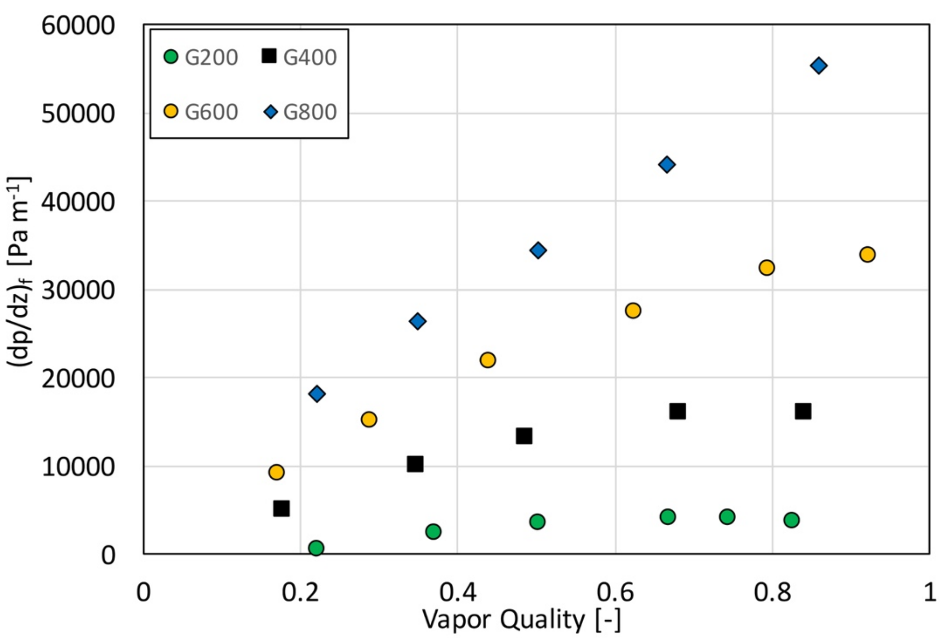

Figure 6: Effect of mass velocity on frictional pressure gradient at an imposed heat flux of 60 kW m^{-2}. G expressed in [kg m^{-2} s^{-1}].

Similar considerations can be drawn when considering the results plotted in Figure 5b, there is not any noticeable effect of the heat flux up to *HF*=30 kW m^{-2}. The heat transfer coefficient measured at *HF*=15 kW m^{-2} and *HF*=30 kW m^{-2} are almost similar and they increase with vapor quality. The two-phase forced convection seems to control the boiling process. When comparing the data measured at higher heat fluxes with that for G=400 kg m^{-2} s^{-1} (Figure5a), it can be stated that due to the high mass velocity, the plateau where the heat flux can be considered almost constant slightly recedes to lower vapor quality, meaning that that the nucleate boiling is quickly overcome by the convective boiling heat transfer mechanism. In this case, the heat transfer coefficients measured at *HF*=90 kW m^{-2} are higher than those measured at lower heat fluxes. This confirms what highlighted before and also stated by Mancin *et al*. (2015), i.e. it seems that there is a mass velocity range (G=200-400 kg m^{-2} s^{-1}), in which the favorable characteristics of the helical microfin tube are even more pronounced leading to very high boiling heat transfer performance.
The experimental frictional pressure gradients are plotted in Figure 6 as a function of the mean vapor quality, for the sake of clarity, only data relative to an imposed heat flux of 60 kW m^{-2} is reported. As described before, the homogeneous model was considered to estimate the momentum pressure drops, which were subtracted from the total measured pressure drops. The results show that, at constant mass velocity, the frictional pressure gradient increases with vapor quality. Furthermore, at constant vapor quality, the frictional pressure gradient increases as the mass velocity increases.

4. CONCLUSIONS

The paper presents experimental heat transfer coefficients and pressure drops measured during flow boiling inside a mini microfin tube with an inner diameter at the fin tip of 4.3 mm. Tests were run at a constant saturation temperature of 30 °C at the inlet of the test section, by varying the vapor quality from 0.1 to 0.95, the mass velocity from 100 to 800 kg m^{-2} s^{-1}, and the heat flux from 15 to 90 kW m^{-2}. The results confirm that the heat transfer process is controlled by the two mechanisms that govern the flow boiling phenomenon, i.e. nucleate boiling and two-phase forced convection, and that the prevailing one depends upon the actual operating test conditions.
In general, it can be stated that at low heat flux, the heat transfer coefficient is highly affected by vapor quality, meaning that the convective boiling dominates the flow boiling phenomenon. A different situation occurs at high heat fluxes, where the heat transfer coefficient is not affected by mass velocity and weakly affected by vapor quality, meaning that the phase change process is mainly controlled by nucleate boiling. The two-phase frictional pressure drops were also measured. They increase with both mass velocity and vapor quality. Finally, the results highlight the promising heat transfer capabilities of mini microfin tubes during flow boiling; nevertheless, additional heat transfer measurements with different tube diameters, different helical geometries, and different type of refrigerants are surely needed.

NOMENCLATURE

A	area	(m^2)
c_p	specific heat capacity	(J kg^{-1} K^{-1})
D	fin tip diameter	(m)
G	mass velocity	(kg m^{-2} s^{-1})
h	fin height	(m)
HTC	heat transfer coefficient	(W m^{-2} K^{-1})
HF	heat flux	(W m^{-2})
J	specific enthalpy	(J kg^{-1})
k	coverage factor	(-)
I	electrical current	(A)
L	heated length	(m)
$\dot{m}$	mass flow rate	(kg s^{-1})
n	fin number	(-)
p	pressure	(Pa)
P_{EL}	electrical power	(W)
q	heat flow rate	(W)
s	thickness	(m)
t	temperature	(°C)
v	specific volume	(m^3 kg^{-1})
x	vapor quality	(-)

Δp	pressure drop	(Pa)
Δt	temperature difference	(°C)
ΔV	electric potential	(V)
Δx	vapor quality change	(V)
β	helix angle	(°)
γ	apex angle	(°)
λ	thermal conductivity	(W m^{-1} K^{-1})
Subscript		
a	momentum	
c	gravity	
evap	evaporator	
i	i-th	
in	inlet	
f	frictional	
L	liquid	
loss	loss	
out	outlet	
r	refrigerant	
sat	saturation	
sub	subcooled liquid	
TS	test section	
V	vapor	
w	water	
wall	wall	

REFERENCES

Diani, A., Mancin, S., Rossetto, L., 2014, R1234ze(E) flow boiling inside a 3.4 mm ID microfin tube, *Int J. Refrig*., vol. 47: p. 105-119.

Diani, A., Mancin, S., Rossetto, L., 2015a. Flow boiling heat transfer of R1234yf inside a 3.4 mm ID microfin tube, *Experimental Thermal and Fluid Science*, vol. 66: p. 127–136.

Diani, A., Mancin, S., Cavallini, A., Rossetto, L., 2015b. R1234ze(E) Flow Boiling Heat Transfer and Pressure Drop Inside a 2.4 mm Microfin Tube, *Proc. of ICR 2015*, August 16 - 22 - Yokohama, Japan, Paper 549.

Diani, A., Rossetto, L., 2015, Vaporization inside a mini microfin tube: experimental results and modeling, *Journal of Physics: Conference Series*, vol. 655: p. 012032.

Fujie, K., Itoh, N., Kimura, H., Nakayama, N., Yanugi, T., 1977, *Heat transfer pipe*, US Patent 4044797, assigned to Hitachi.

Kline, S.J., McClintock, F.A., 1953. Describing uncertainties in single-sample experiments. *Mech. Eng*., vol. 75: p. 3–8.

Kondou, C., BaBa, D., Mishima, F., Koyama, S., 2013, Flow boiling of non-azeotropic mixture R32/R1234ze(E) in horizontal microfin tubes, *Int. J. Refrig.,* vol. 36: p. 2366-2378.

Kondou, C., Mishima, F., Liu, J.F., Koyama, S., 2014a. Condensation and Evaporation of R744/R32/R1234ze(E) Flow in Horizontal Microfin Tubes, *Proc. of International Refrigeration and Air Conditioning Conference at Purdue*, West Lafayette, IN, USA, Paper 1448.

Kondou, C., Mishima, F., Liu, J.F., Koyama, S., 2014b. Condensation and Evaporation of R134a, R1234ze(E) and R1234ze(Z) Flow in Horizontal Microfin Tubes at Higher Temperature, *Proc. of International Refrigeration and Air Conditioning Conference at Purdue*, West Lafayette, IN, USA, Paper 1446.

Lemmon, E.W., Huber, M.L., McLinden, M.O., 2013, *NIST Standard Reference Database 23: Reference Fluid Thermodynamic and Transport Properties- REFPROP, Version 9.1*, National Institute of Standards and Technology, Standard Reference Data Program, Gaithersburg.

Mancin, S., Diani, A., Rossetto, L. 2015. Experimental Measurements of R134a Flow Boiling Inside a 3.4-mm ID Microfin Tube (2015) *Heat Transfer Engineering*, vol. 36, (14-15): p. 1218-1229.

ACKNOWLEDGEMENT

The support of Wieland-Werke AG and of Dr. Christoph Walther on this research activity is gratefully acknowledged. Generalmeccanica Snc and Dr. Damiano Soprana are gratefully acknowledged for their valuable help in the manufacturing of the test section.